The European Physical Journal Plus

# Lowering cement clinker: A thorough, performance based study on the use of nanoparticles of SiO2 or montmorillonite in Portland limestone nanocomposites

--Manuscript Draft--

| | |
|---|---|
| **Manuscript Number:** | EPJP-D-18-01060R2 |
| **Full Title:** | Lowering cement clinker: A thorough, performance based study on the use of nanoparticles of SiO2 or montmorillonite in Portland limestone nanocomposites |
| **Article Type:** | Regular Article |
| **Corresponding Author:** | Styliani Papatzani, PhD, MSc, MSc/DIC<br>University of Brighton - Moulsecoomb Campus<br>UNITED KINGDOM |
| **Corresponding Author Secondary Information:** | |
| **Corresponding Author's Institution:** | University of Brighton - Moulsecoomb Campus |
| **Corresponding Author's Secondary Institution:** | |
| **First Author:** | Styliani Papatzani, PhD, MSc, MSc/DIC |
| **First Author Secondary Information:** | |
| **Order of Authors:** | Styliani Papatzani, PhD, MSc, MSc/DIC |
| | Kevin Paine, PhD |
| **Order of Authors Secondary Information:** | |
| **Funding Information:** | FP7 Ideas: European Research Council (262954) — Dr Kevin Paine |
| **Abstract:** | Nanotechnology has changed the way we perceive science, our world and consequently the built environment. Cement sustainability, is of primary importance and nanotechnology can offer new alternatives towards the lowering the CO2 footprint by reducing clinker, by increasing the by-products content and by creating more durable formulations. This paper presents an optimization protocol of ternary Portland limestone nanocomposites through the addition of nanosilica or nanomontmorillonite (nMt) particles. Thermal gravimetric and X-ray diffraction analyses, confirmed the Ca(OH)2 consumption towards the production of C-S-H. Mercury intrusion porosimetry ((MIP) and long term relative density measurements coupled with field emission scanning electron imaging (FESEM) confirmed the microstructural changes leading to strength enhancement. Lastly, limitations were determined through the extensive study of the addition of nanosilica particles at four different dosages (0.1, 0.5, 1.0, 1.5% addition by total mass of solids) or three different nMt dispersions at five different dosages (0.5, 1.0, 2.0, 4.0 and 5.5%). Strength tests and characterization were carried out at day 1, 7, 28, 56, 90 and 170 to assess both the short and long term effects. Nanosilica and inorganic nMt particles were found to be the most effective at lower dosages for strength, hydration and microstructural improvements. |

# Lowering cement clinker: A thorough, performance based study on the use of nanoparticles of $SiO_2$ or montmorillonite in Portland limestone nanocomposites

Styliani Papatzani[*,1,2] and Kevin Paine[3]

[*,1] Corresponding author: Hellenic Ministry of Culture, Directorate of Restoration of Medieval & Post-medieval Monuments, Tzireon 8-10, 11742, Athens, Greece, spapatzani@gmail.com

[2] School of Environment and Technology, University of Brighton, BN2 4GJ, Brighton

[3] BRE Centre for Innovative Construction Materials, University of Bath, BA2 7AY, Bath, UK, k.paine@bath.ac.uk

## Abstract

Nanotechnology has changed the way we perceive science, our world and consequently the built environment. Cement sustainability, is of primary importance and nanotechnology can offer new alternatives towards lowering the $CO_2$ footprint by reducing clinker, by increasing the by-products content and by creating more durable formulations. This paper presents an optimization protocol of ternary Portland limestone nanocomposites through the addition of nanosilica or nanomontmorillonite (nMt) particles. Thermal gravimetric and X-ray diffraction analyses, confirmed the $Ca(OH)_2$ consumption towards the production of C–S–H. Mercury intrusion porosimetry ((MIP) and long term relative density measurements coupled with field emission scanning electron imaging (FESEM) confirmed the microstructural changes leading to strength enhancement. Lastly, limitations were determined through the extensive study of the addition of nanosilica particles at four different dosages (0.1, 0.5, 1.0, 1.5% addition by total mass of solids) or three different nMt dispersions at five different dosages (0.5, 1.0, 2.0, 4.0 and 5.5%). Strength tests and characterization were carried out at day 1, 7, 28, 56, 90 and 170 to assess both the short and long term effects. Nanosilica and inorganic nMt particles were found to be the most effective at lower dosages for strength, hydration and microstructural improvements.

**Keywords:** Nanosilica, nanomontmorillonite, low-clinker-cements, optimization, Portland limestone nanocomposites, TGA, XRD, strength tests, MIP, relative density, FESEM.

## 1. Introduction

There is a worldwide concern with regards to the $CO_2$ emissions, and cement industry through the clinkering process is responsible for approximately 8% of the $CO_2$ emitted globally. The $CO_2$ footprint is primarily attributed to the decalcination of limestone, the fuel and the electricity consumed for the clinkering process. Cement scientists, therefore, are focusing on the replacement of Portland cement by other supplementary cementitious materials in order to reduce the $CO_2$ footprint. In light of this, the European Union has specified 27 cement formulations, based on different compositions. Of these, Portland limestone cements are amongst the most broadly used in Europe. In fact, for "CEMII/A-L" cements, i.e. for non-pozzolanic cements, the upper limit of limestone content ranges from 6% to 20% by total mass of binder, while the permissible clinker content lies within 80-95% by total mass of binder, as specified by the Eurocodes [1]. Similarly, USA and Canada have also recently standardised the use of up to 15% interground limestone in Portland limestone cements (codes ASTM C595-M-2015 and CSA A3001-2010, respectively). Globally, the limestone additions range from 10% to 35% in national and international standards, as is reviewed in Elgalhud et al.[2].

The worldwide effort conducted to reduce Portland cement content is recorded in a number of published papers on the effect of limestone addition on concrete properties; Elgalhud et al. [2], after reviewing 171 publications since 1993, suggested that although up to 25% of limestone addition does not impair the pore structure of concrete, strength may be affected by additions of limestone exceeding 15% by mass of binder. In fact, a study on the parameters affecting Portland limestone cements conducted by Tsivilis et al. [3] established that increasing the limestone content to 35% by mass of binder causes a significant strength loss.

Similarly, Lollini et al. [4] who studied the mechanical properties and the resistance to chloride penetration of Portland limestone concrete specimens concluded that both properties deteriorated at 15% limestone replacement. A

further decrease was noted at 30% limestone replacement at different water-to-binder ratios; 0.62, 0.46, 0.42 with the use of an acrylic superplasticizer.

It is well established that the formation of monocarboaluminates as fillers in cement can make the concrete microstructures denser by reacting with $C_3A$, while limestone providing nucleation sites can accelerate hydration. However, at higher limestone additions, the volume of hydrates decreases, causing a drop in compressive strength due to the dilution of clinker phases by limestone [5]. In addition to this, the large surface area of cement clinker is found to be more effective in enhancing strength than that of limestone. For this, the 15% threshold for limestone addition seems to gain a consensus amongst scientists irrespective of the fineness of the limestone powder [2,6].

Recently, studies are beginning to look into possibilities of increasing the limestone content beyond the 15% threshold. Amongst these possibilities include the use of nanotechnology, where nanoparticles are being added alongside limestone to PC-limestone blends. Several studies have investigated the effect silica nanoparticles (nano-$SiO_2$, abbreviated as nS) and nano-montmorillonite (abbreviated as nMt) nanoparticles have on various cement formulations, containing three or four constituents [7–9]. For example, with respect to nS, researchers propose dosages ranging from 0.5% [10], to 1% [10,11] and even 10% by mass of cement [12]. With respect to nMt, optimum content determination is more vague as the procedure for nMt production can greatly affect the end product [13]. The effect of the addition of these nanoparticles on ternary PC-limestone cements is yet to be investigated in terms of the optimum dosage and modification of properties.

Adding to this, the strength and durability of concrete is governed by the structure of C–S–H gel, which is the major component in the hydrating and hardened cement paste [14]. Nanosilica or in other words nanosized silica, comprises of Si atoms connected with four atoms of oxygen, creating tetrahedra, the basic building block. These Si atoms are unsaturated on their outer side, allowing for reactions with water leading to the creation of silanol groups (=Si–OH), governing adsorption and surface reactivity of silica [13].

As for the nanomontmorillonites, they are developed from montmorillonites (MMT) and several factors have contributed to the popularity of MMT in cement science:

(i) its vast surface area 10 to 800 $m^2/g$ [15,16]. It is well known that the greater the available surface area for reactions, the greater the amount of C–S–H formed during cement hydration;

(ii) its naturally occurrence; MMT is a relatively abundant mineral;

(iii) its nanostructure is formed by layers of platelets, composed of a sheet of octahedra of $Al_2O_6$, sandwiched at the top and bottom by a sheet of tetrahedra of $SiO_2$, therefore already exhibits an inherent abundance in Si and Al. The total thickness of this 2:1 ratio structure is approximated to lie in the range of 0.95 nm to 1 nm [17];

(iv) MMT exhibits high cation exchange capacity in the order of 80 to 120 meq/100g [18], hence higher degree of expansion due to ionisation of the structure upon hydration. This separation of the individual layers allows for the dispersion of the platelets and the 'nano-effect' – high aspect ratio, high surface area – can be realised. The effect the various dispersing agents have on the nanostructure of nMt has already been extensively investigated [19].

Health and safety issues must also be considered and several guides have been published to cover these issues [20–22]. The European Agency for Safety and Health at Work has also published a number of legislative documents on the risks related to the use of nanomaterials in the workplace; Framework Directive 89/391/EEC, the Chemical Agent Directive 98/24/EC and the Carcinogen and Mutagen Directive 2004/37/EC. As far as the cost is concerned, the price of amorphous nanosilica powder ranges between 1.4 to 5 USD per kilogram, while colloidal nanosilica suspension in water costs 110 USD for the 4-litre bottle [23]. Industrial nanomontmorillonite typically costs 70 USD per 0.5 kg.

In this study, the envelope was pushed further with the total limestone content of the reference paste being reduced to 40% by mass, while the clinker content of the reference paste was equal to 60% by total mass of binder, which accounts to an almost 30% reduction of the lower bound of clinker in Portland limestone cements. This very low clinker content was achieved with the use

of various nanoparticles; an aqueous nS dispersion, abbreviated as LnS and three different nMt dispersions.

This paper presents an optimization protocol of ternary Portland limestone - nanosilica or nanomontmorillonite (nMt) nanocomposites. The LnS or nMt dispersion was added at different proportions resulting eventually, in a total of four LnS enhanced cementitious nanocomposite formulations and fifteen, nMt enhanced cementitious nanocomposite formulations. Specimens were prepared according to the specifications given in literature [9]. Characterization of selected pastes allowed for more conclusions to be drawn and links to be formed between nanostructural characteristics and mechanical performances. For the first time:

(i) the effectiveness of the various nanoparticles was compared, including nanosilica and nanomontmorillonite. Further to this, this is the first study recording the effect of inorganic nMt in Portland-limestone formulations

(ii) compressive strength, additional pozzolanic or hydraulic activation, C–S–H formation, porosity and late age density were interrelated as performance indicators.

(iii) limitations were determined relating to the nanoparticle dosage and suggestions were made for further improvements towards more sustainable cement formulations.

## 2. Materials and Methods

### 2.1 Materials

The materials used were:

- Portland limestone cement CEMII/A-L42.5, with a limestone content of 14%, conforming to EN 197-1. The Portland cement (PC) content 86% by mass was considered separately from the limestone (LS) content (14% by mass), in order to be able to adjust the total limestone content of the composite binders. According to the supplier clinker is composed of: 70% $C_3S$, 4% $C_2S$, 9% $C_3A$, 12% $C_4AF$.
- Limestone (additional), conforming to EN 197-1. The total LS content was assigned to each paste.

The nanomaterials used were:

- Colloidal amorphous LnS in an aqueous suspension containing about 30% by mass of LnS particles - The particle size of the LnS in the colloidal solution was further investigated by transmission electron microscopy (TEM) as described in literature [7]. TEM analysis showed that the diameter of the particles ranged from 8 nm to 50 nm and that they were homogenously dispersed.
- Organomodified nanomontmorillonite aqueous dispersion (nC1) containing 15% by mass nMt solids, 5% by mass (non-ionic) fatty alcohol and 1% by mass defoaming agent [19,24].
- Organomodified nanomontmorillonite aqueous dispersion (nC2) containing 15% by mass nMt solids and 5 % by mass (anionic) alkyl aryl sulphonate [19,24].
- Inorganic nanomontmorillonite aqueous dispersion (nC3) containing 15% by mass nMt solids and inorganic sodium montmorillonite [19,24].

## 2.2 Methods

### 2.2.1. Mix design

A non-pozzolanic formulation PC60LS40 was used as the reference to investigate whether the addition of LnS has a pozzolanic effect. In this reference paste, PC refers to the net amount of Portland cement and LS refers to the amount of total limestone content. The amount of water present in the LnS aqueous solution was subtracted from the total amount of water in the mix, in order to maintain a constant water to binder ratio (w/b) of 0.3. The PC content was kept constant and the content of LnS solids was deducted from the LS content. This was done to keep the $Ca(OH)_2$ production during PC hydration comparable in all pastes, so as to detect possible pozzolanic reactivity of the nanoparticles (in terms of $Ca(OH)_2$ consumption).

Therefore, the general formula for the LnS modified pastes was:

$$PC(60) + LS(40 - x) + LnS(x) \qquad \text{Equation: -1}$$

Where $x$ = % by mass of LnS solids, ranging from 0 to 1.5%.

The mix proportions in terms of the per cent amount of the total mass of binder are shown in Table 1.

Table 1: LnS or nMt modified ternary formulations - Mix proportions % by total mass of solids

| Sample | PC (%) | LS (%) | LnS (%solids) | nMt (%solids) | W/B |
|---|---|---|---|---|---|
| **PC60LS40+0%LnS** | 60 | 40.0 | 0.0 | 0.0 | 0.3 |
| **PC60LS39.9+0.1%LnS** | 60 | 39.9 | 0.1 | 0.0 | 0.3 |
| **PC60LS39.5+0.5%LnS** | 60 | 39.5 | 0.5 | 0.0 | 0.3 |
| **PC60LS39+1.0%LnS** | 60 | 39.0 | 1.0 | 0.0 | 0.3 |
| **PC60LS38.5+1.5%LnS** | 60 | 38.5 | 1.5 | 0.0 | 0.3 |
| **PC60LS40+0% nMt** | 60 | 40 | 0.0 | 0.0 | 0.3 |
| **PC60LS39.5+0.5% nMt** | 60 | 39.5 | 0.0 | 0.5 | 0.3 |
| **PC60LS39+1.0% nMt** | 60 | 39.0 | 0.0 | 1.0 | 0.3 |
| **PC60LS38+2.0% nMt** | 60 | 38.0 | 0.0 | 2.0 | 0.3 |
| **PC60LS36+4.0% nMt** | 60 | 36.0 | 0.0 | 4.0 | 0.3 |

Fifteen ternary cement combinations were designed for the nMt nanoparticles. This comprised of Portland limestone cement, limestone, and either of the two organomodified nMt dispersions or the inorganic nMt dispersion. The non-pozzolanic paste PC60LS40, containing only PC and LS, was again selected as the control mix, to investigate whether the addition of any of the nMt dispersions has a pozzolanic effect. The content of nMt solids ranged from 0%, 0.5%, 1%, 2%, 4% and 5.5% by mass. The 5.5% represented the upper limit of nMt addition in the cement paste, as the water used in the nMt dispersion was considered as available to react during the hydration of

cement and therefore was deducted from the total amount of water to be added according to the w/b ratio which again was constant and equal to 0.3. Furthermore, PC content was kept constant and the content of nMt solids was deducted from the LS content for the reason mentioned above. Therefore, the general formula of the matrix of the ternary cement paste mixes was:

$$PC(60) + LS(40 - x) + nMt(x) \qquad \text{Equation: -2}$$

Where $x$ = % by mass of nMt solids ranging from 0 to 5.5%.

The mix proportions in terms of per cent content of the total mass of binder are also shown in Table 1.

The mix design procedure for the non-pozzolanic reference pastes is described in literature [25] as well as the methodology governing the mixing procedure, casting, curing and demoulding [26]. The nanoparticles of silica have been characterized elsewhere [27] as well as the nanomontmorillonite dispersions [19,24].

### 2.2.2. Characterization techniques

Preparation of materials: For the characterization of the pastes, arrest of hydration was performed following two different methodologies. In brief, if images were to be generated and the microstructure to be evaluated via FESEM and MIP, solvent exchange was the technique employed for the arrest of hydration. The samples were crushed and immersed in isopropanol for 48 hours. Isopropanol was selected as the most appropriate solvent according to Zhang and Scherer and Bye [28,29]. The samples were, then, vacuum dried for 24 hours. For experiments in which chemical reactions would occur or where the chemical composition had to be evaluated, such as TGA, XRD, the oven drying technique was adopted as explained in detail in Calabria-Holley et al. [27].

**Compressive strength tests**: Compressive strength tests were carried out on up to six cylindrical specimens per mix. All samples were tested at a loading speed of 0.5MPa/s. The value of strength was obtained from the mean of the specimens tested and therefore, the compressive strength results refer to mean compressive strength measured.

**Thermal gravimetric analyses (TGA):** Thermal gravimetric analyses (TGA) were carried out using a Setaram TGA92 instrument. 20 mg of each sample were placed in an alumina crucible and heated at a rate of 10°C/min from 20°C to 1000°C under 100 mL/min flow of inert nitrogen gas. Three different areas were distinguished; as described in literature and correspond to the hydrates produced and consumed [26]:

(i) The first one is related to the dehydration of C–S–H, ettringite, gehlenite and monosulfate, between 100ºC and 200ºC.

(ii) The second area of interest is associated with the dehydration of $Ca(OH)_2$ between 440ºC and 510ºC.

(iii) The third area of interest is the decomposition of $CaCO_3$ occurring between 700ºC and 810ºC.

**X-Ray diffraction (XRD):** Powder flat plate XRD measurements were performed using a D8 ADVANCE x-ray diffractometer with $CuK_\alpha$ radiation controlled by a Dell PC. Spectra were obtained in the range $4^o < 2\theta < 60^o$. Analysis of peaks and d-spacing [according to Bragg's law ($n\lambda = 2d\sin\theta$) (Ramachandran and Beaudoin, 2001)] was carried out using EVA software.

**Long-term relative density of cementitious nanocomposites:** BS EN 12390-7:2000, was selected as a basis for the long-term relative density measurements of the hardened pastes. The exact procedure is presented in literature [26].

**Mercury Intrusion Porosimetry (MIP):** The mercury intrusion porosimeter used was an Autopore III - Model unit 9420 supplied by Micromeritics, Hexton, Herts, UK. Stems of 3 ml capacity were filled with the vacuum dried solids of the arrested hydration paste and low pressure analysis was carried out.

**Field emission electron microscopy (FESEM):** Secondary electron imaging of the pastes was generated using a field emission electron microscope (FESEM) Jeol JSM 6301F at 2.4 kV, spot size of 7 and working distance of 16 mm. The specimens were sputter coated with a layer of chromium 5 nm thick using Quorum Q 150T. FESEM allowed capturing images at low voltage and high analysis, and indeed was the only microscope with the help of which the nMt were distinguished.

### 2.2.3. Mathematical elaboration

**Correlating hydration characteristics with mechanical strength performance in cementitious nanocomposites:** The high correlation between the consumption of calcium hydroxide towards the formation of hydration products (microscale characteristics) and the delivered compressive strengths (macroscale performance) of the nanosilica modified pastes with respect to time has been already explored in polycarboxylate nanosilica cementitious nanocomposites [26]. This ratio is further validated by the ternary formulations presented in this paper.

## 3. Results and discussion

### 3.1 Compressive strength of cementitious nanocomposites

### 3.1.1. Nanosilica (LnS) addition

One of the reasons for which cement pastes with higher nS contents were designed, was to maximize homogeneity within the pastes. This was expected to minimise the standard deviation (stdv) of compressive strength. The stdv was more significant for the two extreme LnS contents (in the order of 6.6 MPa) and lower for the 0.1% LnS content (approximately 4.9 MPa). The values of stdv are not shown in Figure 1 for reasons of clarity, but are included in Table 2.

Table 2: Standard deviation of compressive strength results of all formulations at different ages

| | STANDARD DEVIATION | | | | | | | |
|---|---|---|---|---|---|---|---|---|
| | 1 Day | 7 Days | 28 Days | 56 Days | 90 Days | 180 Days | | |
| PC60LS40 | 5,63 | 4,33 | 8,95 | 12,07 | 11,82 | 2,8 | | min & max of stdv |
| PC60LS39.5+0.5%nC1 | 3,6 | 2,5 | 1,8 | 3,0 | 2,3 | 2,0 | nC1 min | 1,7 |
| PC60LS39+1%nC1 | 2,3 | 3,5 | 5,9 | 1,8 | 4,1 | 3,6 | nC1 max | 7,4 |
| PC60LS38+2%nC1 | 5,2 | 1,9 | 7,2 | 6,0 | 7,4 | 7,3 | nC1 Av | 3,0 |
| PC60LS36+4%nC1 | 1,7 | 5,0 | 4,7 | 3,0 | 4,3 | 3,0 | | |
| PC60LS34.5+5.5%nC1 | 2,2 | 2,1 | 4,3 | 2,5 | 2,8 | 2,2 | | |
| PC60LS39.5+0.5%nC2 | 1,8 | 2,1 | 1,1 | 2,0 | 6,5 | 1,9 | nC2 min | 0,3 |
| PC60LS39+1%nC2 | 2,3 | 3,3 | 4,9 | 0,3 | 6,6 | 4,9 | nC2 max | 8,8 |
| PC60LS38+2%nC2 | 5,0 | 3,8 | 4,1 | 8,8 | 3,7 | 0,4 | nC2 Av | 3,3 |
| PC60LS36+4%nC2 | 2,9 | 5,3 | 6,5 | 3,6 | 7,5 | 6,9 | | |
| PC60LS34.5+5.5%nC2 | 1,5 | 0,7 | 2,6 | 1,8 | 2,0 | 3,3 | | |
| PC60LS39.5+0.5%nC3 | 7,1 | 4,1 | 4,9 | 4,2 | 2,4 | 7,3 | nC3 min | 0,4 |
| PC60LS39+1%nC3 | 0,7 | 5,4 | 5,4 | 10,7 | 0,4 | 18,1 | nC3 max | 18,1 |
| PC60LS38+2%nC3 | 0,5 | | 2,9 | 9,7 | 6,5 | 2,8 | nC3 Av | 4,1 |
| PC60LS36+4%nC3 | 1,0 | 3,9 | 1,5 | 2,0 | 2,9 | 3,6 | | |
| PC60LS34.5+5.5%nC3 | 0,6 | 6,5 | 5,3 | 10,5 | 2,9 | 7,1 | | |
| PC60LS39.9+0.1%LnS | 5,2 | 7,7 | 6,4 | 6,7 | 10,5 | 5,5 | LnS min | 5,2 |
| PC60LS39.5+0.5%LnS | 6,1 | 9,6 | 6 | 9 | 14,1 | 1,5 | LnS max | 10,5 |
| PC60LS39+1.0%LnS | 5,3 | 4,9 | 4,9 | 2,9 | 4,8 | 7,3 | LnS Av | 6,1 |
| PC60LS38.5+1.5%LnS | 9,9 | 11,6 | 2,6 | 2,2 | 10,7 | 5,5 | | |

Figure 1A shows the effect of LnS on compressive strength for all pastes as measured between day 1 and day 170. According to published research discussed in the introduction section, the compressive strength of Portland limestone cements is inversely related to the LS content. Therefore, the more

the LS the less strong the cement paste at all ages [30]. The addition of LnS led to an improvement in compressive strength in all cases when compared to the reference paste PC60LS40. This confirmed that LnS contributed to the early strength gain, with the higher content (PC60LS38.5+1.5% LnS) paste having the highest compressive strength gain at early ages, but the lower strength gain over 56 days of age. The 0.1% LnS pastes exhibited the largest overall gain in compressive strength, which could be attributed to reduced LnS particle friction during mixing at lower nS contents.

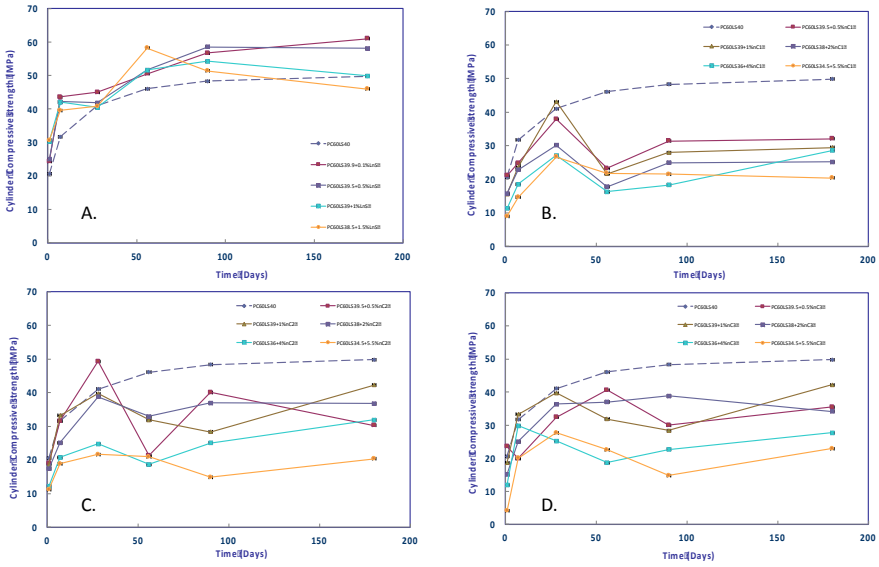


Figure 1. Compressive strength of A. LnS [31], B. nC1, C. nC2 [9] and D. nC3 modified cement pastes.

As shown in Figure 2, the increase in LnS content lead to difficulty in compaction and visible porosity, possibly due to increased particle friction since no superplasticizer was added. Decreased density is, therefore, expected for the highest LnS contents which could possibly cause a reduction in compressive strength.


Figure 2. Uncrushed samples showing porosity due to compaction difficulty with increasing LnS content

Porosity is even more visibly detectable in the crushed specimens as well (Figure 3).

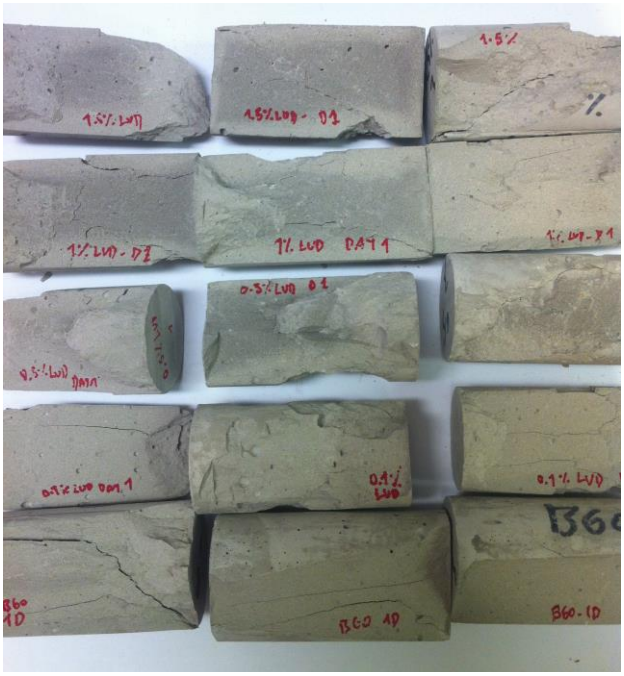


Figure 3. Pictures of visual porosity in crushed specimens modified with LnS

As discussed in the introduction, in past research on PC-limestone cement and concrete formulations different water-to-binder ratios have been investigated at different limestone contents [6,32–35]. The table below offers an overview of the characteristics that affected the performance of these combinations and a comparison between the current research results and the results presented in literature with respect to the highest limestone content combinations. It should be noted that past research on cement pastes was limited to the first 28 days of curing.

Figure 4 offers a comparison between the compressive strength results presented in literature and the improvement that can be attained with the use of nS at 0.5% by mass of binder.

Table 3: Overview of formulation characteristics and compressive strength results presented in literature and in the current research

| | | | Time (Days) | | | | | | | | | |
|---|---|---|---|---|---|---|---|---|---|---|---|---|
| | | | 1 | 2 | 3 | 7 | 28 | 60 | 90 | 180 | 365 | |
| Type | max LS content studied | w/b ratio | Compressive strength (Mpa) | | | | | | | | | Reference |
| Cement | 35% | 0,39 | 9,1 | 17,1 | - | 28,9 | 35,9 | - | - | - | - | [6] |
| Cement | 35% | 0,47 | - | - | 23,8 | 27 | 34,6 | - | - | - | - | [32] |
| Concrete | 20% | 0,37 | - | - | 22 | 32 | 43 | - | 52 | 59 | - | [33] |
| Concrete | 45% | 0,45 | 7 | 11 | - | 21 | 27 | 28,5 | - | 29 | 29 | [34] |
| Concrete | 35% | 0,5 | - | 13,2 | - | 21,3 | 28,7 | - | 35,3 | - | 40,2 | [35] |
| Cement PC-LS | 40% | 0,3 | 20,6 | - | - | 31,7 | 41 | 46 | 48,3 | 49 | - | Current research ref paste |
| Cement PC-LS-0.5%nS | 40% | 0,3 | 25 | - | - | 42 | 42 | 51,6 | 58,2 | 58,1 | - | Current research nS paste |

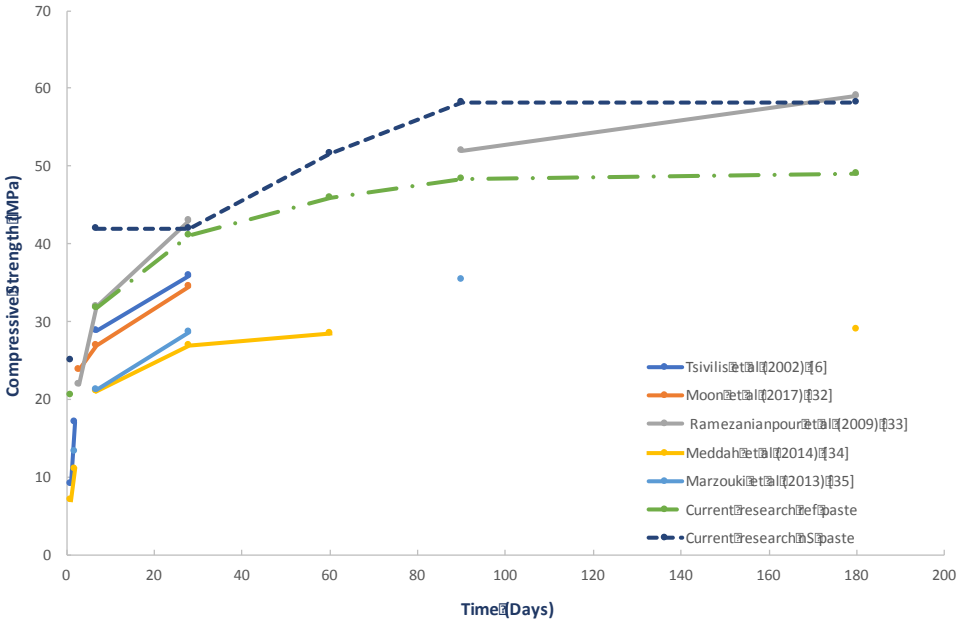


Figure 4. Comparison of compressive strength results in current research and in literature

### 3.1.2 Nanomontmorillonite (nMt) addition

The standard deviation was computed for all specimens but was not presented in the graphs for reasons of clarity. All standard deviation results are presented separately in Table 2. The standard deviation of the reference paste was 8 MPa. For nC1 it was approximately equal to 3 MPa, for nC2 it reached 3.3 MPa, whereas for nC3 it was about 4.1 MPa. Therefore, the addition of nMt seemed to have improved the standard deviation of compressive strength of the reference paste. This is an indication of the better packing that nanomontmorillonite dispersions can offer within Portland limestone cement pastes [13,19], still, however, the addition of nMt did not offer strength improvements. A reason for this relates to the necessity of the use of superplasticizers; As observed in Figure 5, similarly to the highest dosage of LnS, the highest dosages of nMt rendered the mix very stiff and difficult to compact. Superplasticizers would have counteracted this effect; however, they were avoided in order to limit chemical effects from them.

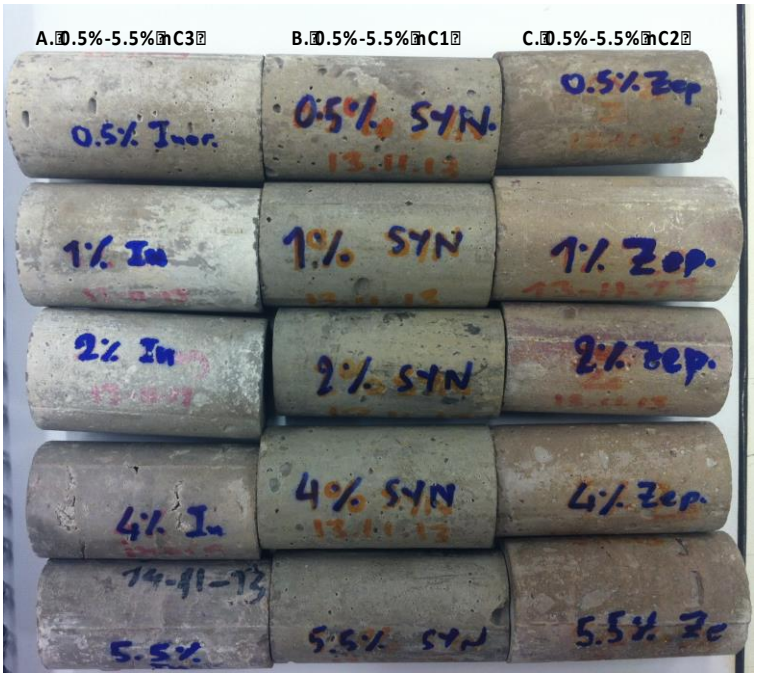


Figure 5. Samples showing porosity due to compaction difficulty with increasing nMt content

The compressive strength results are included in Figure 1B, C, D. All three different nMt dispersions seemed to be offering marginal improvements in compressive strength and only at the lower substitutions, i.e. for nMt solids summing up to 1% by total mass of solids as suggested in earlier studies of binary (Portland cement and organomodified nMT, i.e. not containing limestone) [36]. The performance was less favourable with the advancement of time. By investigating the limits, it was confirmed that high contents of nMt particles, which since in aqueous dispersions, limit the amount of extra water added to the binder, are less favourable to the pastes. At the same time, it can be suggested that 1% of solids is the upper limit for the organomodified nMt with no superplasticizer added, whereas the inorganic nMt could probably be added at slightly greater amounts.

The compressive strength results were in agreement with the nanostructural characterization of the dispersions, presented elsewhere [19]. The overall decrease in compressive strength of the nMt nanomodified pastes, as compared with the reference paste can be attributed to the following factors:

(i) nC1 was identified as the weakest dispersion, with particles conglomerating. Evidently, this led to the creation of lumps of nanomontmorillonite within the paste, acting as weak links and reducing the potentials of variable particle size distribution. Aside from that, nC1 was intercalated, rather than exfoliated, therefore less active as a nanomaterial.

(ii) nC2, which was partly exfoliated with some intercalated platelets, showed less re-agglomeration, better abilities for nanostructural packing and was expected to engage in less brittle behaviour. However, these characteristics were still not enough to improve the compressive strength performance of the nC2 modified pastes beyond the control paste.

(iii) nC3, was better exfoliated and more thermally stable [19], however, very viscous. Hence, the pastes produced at this low w/b ratio were very stiff and this has caused compaction problems (as seen in Figure 5).

(iv) Visual inspection of the crushed specimens (Figure 6), revealed an increase in visual pores for the higher concentrations of nMt, possibly

creating inconsistences within the mass of the nMt modified pastes. Hence, the microstructure of the modified pastes with high nMt content is expected to be more porous.

(v) nC2 and nC3 dispersions were difficult to mix due to their high viscosity, therefore they may have not been homogeneously blended in the hydrating cement paste.

(vi) More mixing time could be prescribed, although the mechanoactivation of the paste could precipitate some water evaporation that could be critical in such pastes.

It is the author's perception that for such low w/b ratio it is possible that the nMt modified cement pastes would perform better and could exploit their potentials with the addition of superplasticizers. This is primarily because it would decrease the thixotropy of the paste permitting: (i) mixing for longer time, (ii) better dispersion of the nanoparticles within the paste, (iii) better compaction, therefore, greater homogeneousness of the paste and (iv) better particle interaction, limiting air voids.

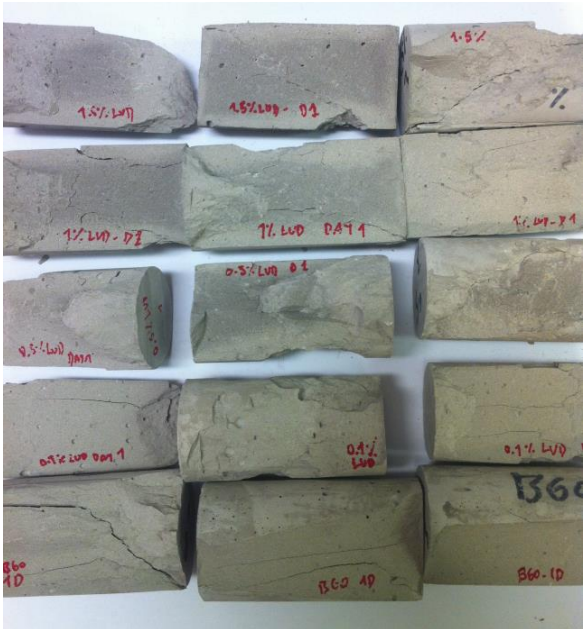


Figure 6. Pictures of visual porosity in crushed specimens modified with nC1/nC2/nC3

### 3.2. Thermal gravimetric and crystallographic analyses of cementitious nanocomposites

#### 3.2.1. Nanosilica (LnS) addition

TGA results can give a clear indication of the amount of $Ca(OH)_2$ consumed towards the production of C–S–H [14,25,26,37,38]. In fact Collier and Lawrence et al. [37,39] have postulated that an increase in the mass loss between 100 and 180°C indicates greater C–S–H and ettringite production whereas the mass loss between 440 and 510°C represents the $Ca(OH)_2$ consumed. TGA results presented in Figure 7, are showing the first temperature range, indicating that the amount of C–S–H present in all LnS enhanced pastes was greater than that in PC60LS40. Hence, it became clear that nS must react with and consume $Ca(OH)_2$ at early ages, including the first 24 hours (Figure 7A), to produce additional C–S–H in these pastes.

With respect to the $Ca(OH)_2$ content (Table 4), for PC60LS40, containing only PC and LS, there was an increase in $Ca(OH)_2$ up to approximately 28 days beyond which it remained constant until day 56, before reducing slightly at day 90 and 170. Interestingly, the $Ca(OH)_2$ at 1 day was equal to 7.9% by mass, and equated to 75% of all $Ca(OH)_2$ produced by the 56-day old paste. Given that the curing conditions did not permit carbonation (no significant increase in calcium carbonate content was observed [25] a fact also confirmed by the XRD as shown in Figure 8. Therefore, it can be argued that for this particular PC, the production of $Ca(OH)_2$ resulting from hydration of alite and belite components of the Portland cement took place rapidly and essentially was completed in the first 28 days, as there was no significant $Ca(OH)_2$ formation after this time. It is worth noting that, $Ca(OH)_2$ consumption amongst the pastes containing over 0.5% LnS was practically the same at day 28, providing further evidence that greater than 0.5% LnS addition will not be able to react in such pastes. Furthermore, consumption of $Ca(OH)_2$ was practically stabilized by 28 days for the 1% LnS addition and by day 56 for the 1.5% LnS addition, providing a first indication of a limit reached. On the contrary, both of the lower LnS additions, the 0.1% and the 0.5%, exhibited a further 33% consumption of $Ca(OH)_2$ at day 170, relative to day 90. Overall, when LnS was present in the paste, the amount of $Ca(OH)_2$ at each age was lower than that of the reference mix (PC60LS40) and the reduction in the $Ca(OH)_2$ content is prominent up to day 28. Given that in PC60LS40 there was no significant $Ca(OH)_2$ formation after 28 days, then it

is reasonable to assume that the colloidal LnS has been converted to C–S–H and that there was no further pozzolanic activity after 28 days for the higher LnS content pastes. The rapid consumption of small proportions of nS has been observed by a number of authors [40,41] and is unsurprising given the high $Ca(OH)_2$/LnS ratio and the high surface area of $SiO_2$ available for reactions.

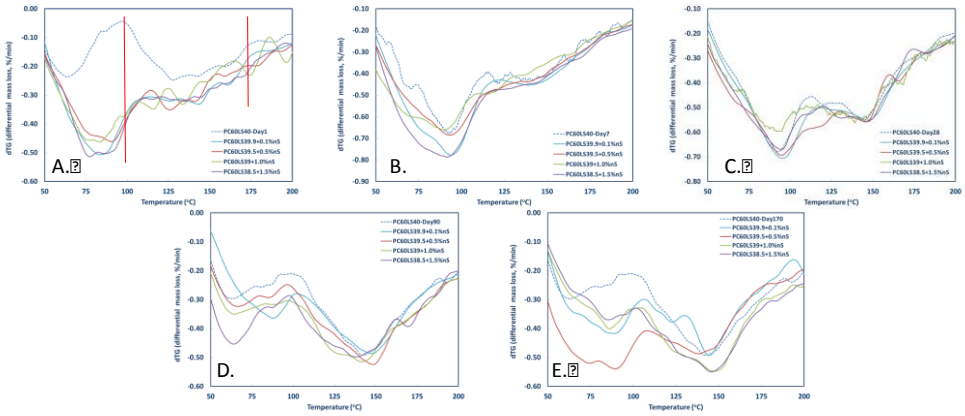


Figure 7. Difference in C–S–H production LnS-enhanced pastes at A. Day 1, B. Day 7, C. Day 28, D. Day 90 and E. Day 170.

Table 4. $Ca(OH)_2$ content of LnS modified cementitious nanocomposites based on PC60LS40

| Time (days) | 1 | 7 | 28 | 56 | 90 | 170 |
|---|---|---|---|---|---|---|
| **Ref-60/40** | 7.9 | 9.1 | 10.3 | 10.6 | 9.0 | 8.8 |
| **PC60LS39.9+0.1LnS** | 7.8 | 9.0 | 10.1 | 10.2 | 9.0 | 8.0 |
| **PC60LS39.5+0.5nS** | 7.2 | 8.6 | 8.8 | 9.0 | 9.0 | 7.0 |
| **PC60LS39+1.0nS** | 6.2 | 6.6 | 8.7 | 9.0 | 9.0 | 8.8 |
| **PC60LS38.5+1.5nS** | 6.4 | 7.9 | 8.6 | 7.7 | 8.0 | 8.0 |

The chemical effect reported due to the presence of high contents of LS in the reference paste, which is the formation of hemicarbonate with a diffraction peak at 10.8°2θ or calcium monocarbonate hydrate with a diffraction peak at 11.7°2θ [30,42] was not seen in the XRD patterns shown in Figure 8. However, the consumption of $Ca(OH)_2$ for the production of C–S–H (hump

marked within red circle) was observed by the XRD as well, although more evident after day 7. Lastly, the immediate reactivity of LnS was also shown in Figure 8, in which the formation of additional C–S–H can be observed at day 1, when the reference paste had no C–S–H to show. The diffracted peak at 9.1°2θ corresponded to ettringite [43].

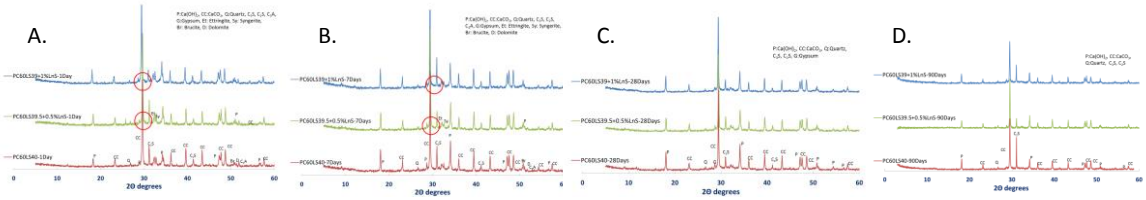


Figure 8. XRD patterns of LnS-enhanced pastes at A. Day 1, B. Day 7, C. Day 28 and D. Day 90.

### 3.2.2. Nanomontmorillonite (nMt) addition

The thermal analyses and crystallographic investigations carried out, showed potential of pozzolanic activity for the three dispersions in their own right (Figure 9). Although, within the cement paste, these analyses are complicated, in Figure 10, the $Ca(OH)_2$ content and the $CaCO_3$ content of selected pastes are shown at different ages. It should be noted that the amount of decomposition of the modifier and nMt were deducted from the mass loss occurring at the 400-500°C temperature band and the amount of decomposing nMt was deducted from the mass loss occurring at the 600-800°C temperature band according to the analyses carried out [19]. It can be maintained that no carbonation has taken place since the lines representing the nanomodified pastes are close and below that of the reference paste (Figure 10B) for most nMt concentrations and ages.

The quantitative analysis is limited by the fact that at 400-500°C the decomposition of both, $Ca(OH)_2$ and modifier, takes place. Therefore, a gas detector on the TG analyser or differential scanning calorimeter would have assisted with the identification of the exact phases decomposing within the specific temperature ranges and therefore the exact mass losses would have been computed. For this reason, further analysis was carried out with respect to the temperature range within which ettringite and C–S–H decompose, i.e.

at approximately 100-130°C for the former and at approximately 125-180°C for the latter. At the same time, it is acknowledged that calcium aluminate hydrates also decompose before 400°C. This comparison is more direct since the percentage of the mass loss of the modifier within this temperature was 2.63% for nC1 and 1.8% for nC2, nC3 lost 5% of adsorbed water in the same temperature range according to the thermal analyses of the vacuum dried dispersions [44]. That is to say, approximately 2% of the solids content (1% to 5.5%) decomposed between 100-180°C. Therefore, the contribution of the mass loss of the modifier can be neglected compared to the mass loss due to the dehydration of ettringite and C–S–H (Minimum contribution of nC to the mass loss between 100-180°C = 1% x 2% = 0.0002 i.e. insignificant).

At Day 1 (Figure 9A), the reference paste contained significant amounts of water which were lost shortly after the 100-125°C temperature range. This excess of water, however, could be captured within the galleries of the nMt and for this reason the mass loss is almost twice that of the reference paste. It should be noted, though that this extra mass loss could be also attributed to the decomposition of the surfactants, however, due to their limited quantity (only 5% by mass of the total quantity of nC) the first hypothesis is more realistic. The results at Day 1 are shown for completion rather than further commenting. It can be seen that in the first 28 days nC2 seemed to have produced more ettringite and C–S–H than the reference paste. Figure 9 shows that by the first 3 months nC3 was the most active, and the greater the amount of nC3, the greater the production of ettringite and C–S–H and nC2 followed at marginally lower mass losses. Figure 9D shows the effect of the nC1/nC2/nC3 at almost half a year since the production of the pastes. It is apparent that the mass losses attributed to ettringite and C–S–H have increased significantly, reaching the highest values amongst the different ages of the pastes. nC3 has a more pronounced activity, which can be explained by the fact that it was better dispersed and less re-agglomerating, therefore the available surface area should be greater than that of the organomodified samples. In general, the TG analyses of the nC1, nC2 or nC3 modified Portland limestone cement pastes (i) confirmed that nC3 could show greater pozzolanic activity and that given the time, nC2 can also engage in pozzolanic reactions.

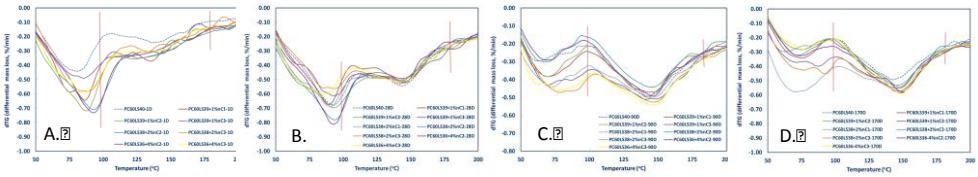


Figure 9. Difference in C–S–H production in nC1/nC2/nC3-enhanced pastes at A. Day 1, B. Day 28, C. Day 90 and D. Day 170.

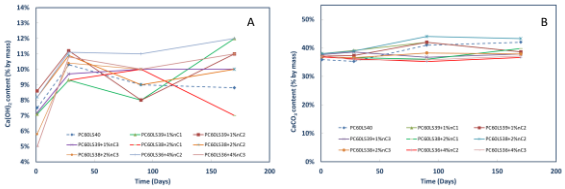


Figure 10. A. $Ca(OH)_2$ and B. $Ca(CO)_3$ content of nC1/nC2/nC3-enhanced cementitious nanocomposites.

Consequently, XRD patterns were developed for nC1, nC2 and nC3 at day 1, 28 and 90 to confirm these findings. As shown in Figure 11 there is a significant reduction in the relative intensity of the $Ca(OH)_2$ peak for all nMt at all ages with respect to the reference paste, contributing to the hypothesis of pozzolanic reactivity of the nMt, in agreement with other studies [45]. The only exception was nC1, whose diffracted peak intensity corresponding to $Ca(OH)_2$ showed an increase at later ages. Moreover, a significant reduction in the relative intensity of the $CaCO_3$ peak can also be noticed, implying that the samples have, indeed, not carbonated.

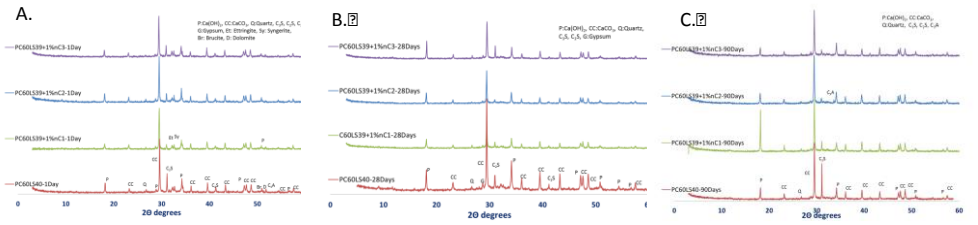


Figure 11. XRD patterns of nC1/nC2/nC3-enhanced pastes at A. Day 1, B. Day 28 and C. Day 90.

### 3.3 Correlating hydration characteristics with mechanical strength performance in nanomodified cementitious nanocomposites

The high correlation between the hydration products (microscale characteristics) and the delivered compressive strengths (macroscale performance) of the nS modified pastes has been proven before [26]. This ratio comprises of the compressive strength of the pastes versus the $Ca(OH)_2$ content, as detected by the TGA. As illustrated in Figure 12 the higher the ratio, the more the related paste outperformed the reference paste. It should be noted that the ratio is particularly sensitive to the homogeneity of the pastes and therefore to micropores and other inconsistences. As an effect, it will only be applied to the LnS (and not nC1/nC2/nC3) cementitious nanocomposites, which were homogeneously dispersed. This elaboration provided a distinct connection between the mechanical performance of the nMt modified pastes and the hydration products formed in these ternary formulations.

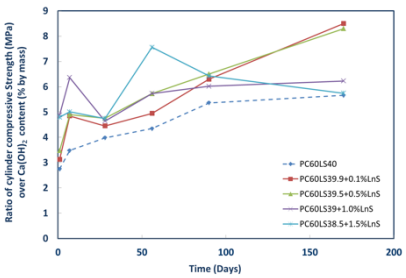


Figure 12. Relating microscale characteristics to macroscale performance of LnS modified cementitious nanocomposites based on PC60LS40

### 3.4. Microstructural characterization of cementitious nanocomposites

#### 3.4.1. Nanosilica (LnS) addition

The microstructure of PC60LS40, PC60LS39.5+0.5%LnS and PC60LS39+1.0%LnS was investigated by field emission scanning electron microscopy at day 28 and 90, which according to the compressive strength analyses (Figure 2) and to the thermal gravimetric analyses (Figure 7) seemed to be the most critical. More micrographs are presented in the Appendix for completion (Appendix Figure 1 and 2).

At day 28 both the PC60LS39.5+0.5%LnS sample (Figure 13A2) and the PC60LS39+1.0%LnS sample (Figure 13A3) exhibited patches of what may be considered denser C–S–H areas compared to the reference paste PC60LS40 (Figure 13A1). Portlandite (P) in the reference paste PC60LS40 (Figure 13A1) is visible in many sites, whereas in the LnS modified pastes fibrillar and honey-comb like C–S–H patches are covering the hydrating cement grains and the Portlandite present in the formulation. At day 90, the intertwined honey comb-like and needle-like hydration products have totally covered the $Ca(OH)_2$ crystals in all pastes (Figure 13B1-3). Furthermore, all voids seem to have been filled by the hydration products and the paste densified even further.

At both day 28 and 90, it is interesting to note, that the morphology observed in PC60LS4060, resembles more PC60LS39.5+0.5%LnS than PC60LS39+1.0%LnS. In the former, the structure is similar to PC60LS40 in terms of visible porosity and amount of Portlandite -$Ca(OH)_2$ crystals, whereas in the latter, the paste looked denser with less $Ca(OH)_2$ crystals present. This indicates that the LnS optimum concentration is approximately 0.5% by total mass of solids, consuming more $Ca(OH)_2$ to form additional C–S–H, an observation correlating well with the formerly presented TGA and compressive strength results. Overall, the LnS enhanced pastes demonstrated a visibly less porous paste.

### 3.4.2. Nanomontmorillonite (nMt) addition

Field emission SEM imaging was also performed on PC60LS39+1%nC1 (Figure 14A1), PC60LS39+1%nC2 (Figure 14A2) and PC60LS39+1%nC3 (Figure 14A3) at day 28 and 90 at 10,000 times magnification. The examination of the microstructure revealed the presence of C–S–H in a nest-like honeycomb morphology, $Ca(OH)_2$ plate crystals (marked by the letter P) and ettringite needle shaped crystals. It is evident that the paste became significantly denser and more homogenized with age with the polygonal crystals being covered with C–S–H lamellae. Age advancement showed lack of coherence, as suspected by the compressive strength tests on that age. nC2 was the more representative hydrophobic nMt dispersion and nC3 the hydrophilic nMt dispersion. As discussed by He and Shi [46] and more recently by Hosseini et al. [47] the high microstructural regularity captured especially by low magnifications especially for nC3 modified pastes is

attributed to the presence of the exfoliated nanomontmorillonite. nC3 modified pastes seemed to have developed the densest morphology, while consuming the $Ca(OH)_2$ crystals. More micrographs are presented in the Appendix for completion (Appendix Figure 1 and 3).

nC2 modified pastes showed a slightly denser paste with greater coherence at day 90 and consumption of $Ca(OH)_2$ crystals. Adding to this, the morphology of the nC2 modified pastes bear close resemblance to the morphologies delivered with the addition of nano-$Al_2O_3$ as shown in the micrographs produced by Hosseini et al. [47]. The reason behind this could be that because nC2 had the highest Si/Al ratio and also the highest Si and Al content [19], the nMt platelets possibly produced greater volume of calcium aluminate hydrates (C–A–H) than of C–S–H.

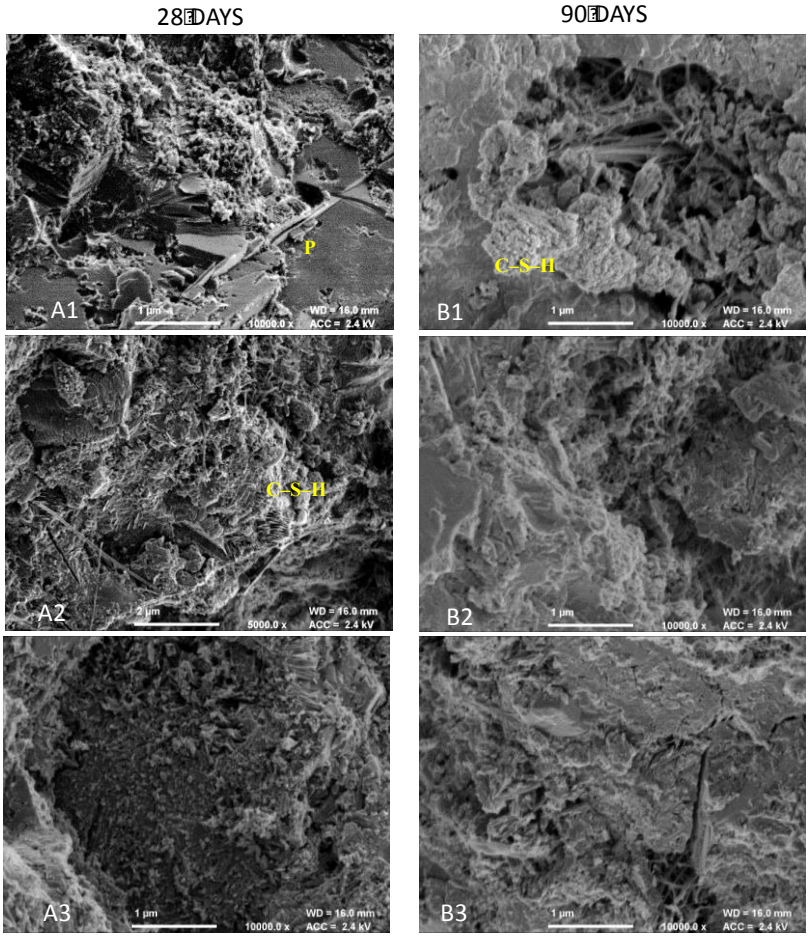


Figure 13. FESEM image of A1. reference paste (PC60LS40) at 28D and B1 at 90D, A2. PC60LS39.5+ 0.5%LnS at 28D and B2 at 90D, A3. PC60LS39+ 1.0%LnS at 28D and B3 at 90D

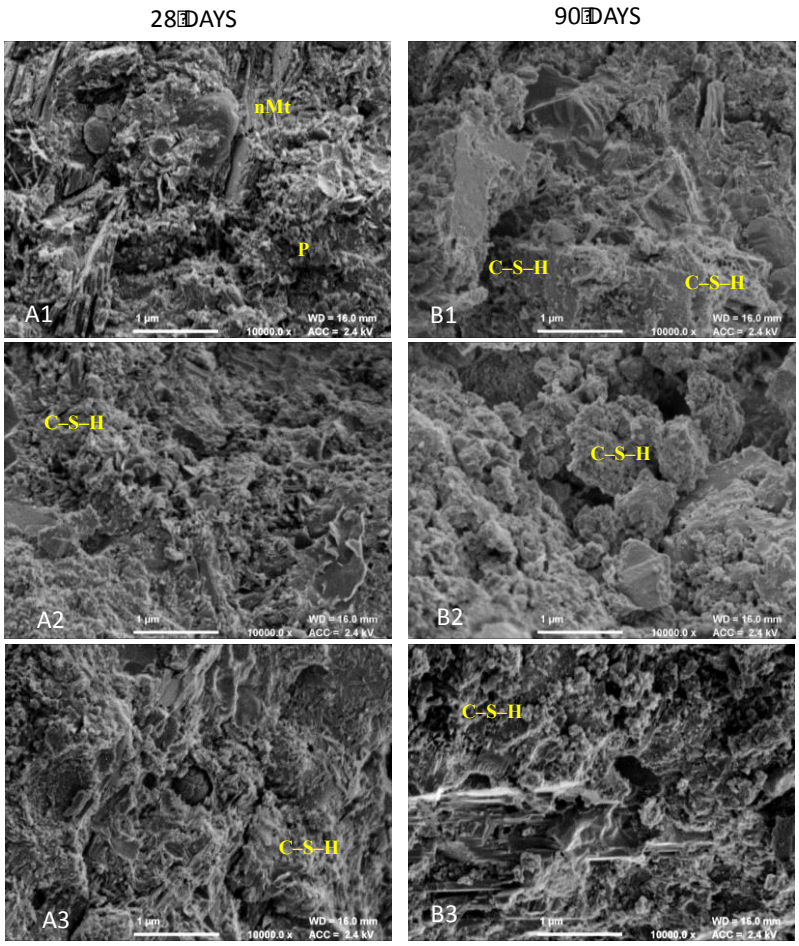


Figure 11. FESEM image of A1. PC60LS39+ 1.0%nC1 at 28D and B1 at 90D, A2. PC60LS39+ 1.0%nC2 at 28D and B2 at 90D, A3. PC60LS39+ 1.0%nC3 at 28D and B3 at 90D (P=portlandite)

### 3.5. Late age relative density and pore structure of cementitious nanocomposites

Knowing that the theoretical density of PC is 3250 kg/m$^3$, that of LS is 2800 kg/m$^3$ and of water 1000 kg/m$^3$ the theoretical density for 60% PC and 40% LS at w/b = 0.3 was found to be equal to 2072 kg/m$^3$. Therefore, judging by

the late age (after month 6) relative density measured (Figure 15A) the reference paste did not seem to contain significant pores. As also discussed with regards to the micrographs the 1.0% LnS modified paste, which seemed to provide denser morphology, also provided the highest relative density, surpassing the reference paste. The next best performance was given by the lower percentage of replacement, bringing together all the analyses presented above. The visual pores observed after the compressive strength tests for the highest LnS content were further justified by Figure 15A. In essence, due to the standard deviation, theoretically, all samples could have the same relative density if the compaction could be optimized. For this, it is the authors' opinion that superplasticizers should be used when higher LnS contents are considered.

Late age density measurements were taken for the nC1/nC2/nC3 modified pastes and discussed elsewhere [48]. Particularly for nC3, which performed best, the measured densities were similar to that of the reference paste for the 0.5% and 1% nC3 addition (Figure 15B). All measurements showed a very low standard deviation, however, again the use of superplasticizers could have reduced the porosity, increasing the density.

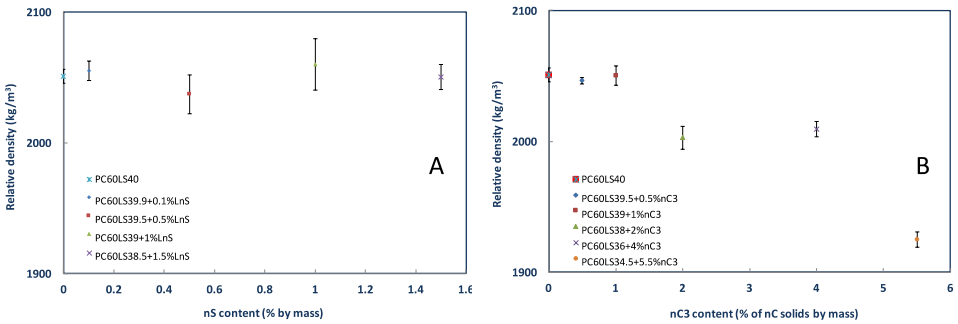


Figure 15. Relative density of LnS or nC3 [48] enhanced cementitious nanocomposites

The accuracy of the MIP has been questioned [49,50] with experimental results suggesting that the MIP, instead of "measuring the size of the pore, is measuring the diameter of the throats, referred as the ink bottle effect". Nonetheless, due to the laboratory equipment limitations, eventually, MIP results were not used as standalone results, but as a means of comparisons with respect to the effect that the three nMt dispersions had on (i) the total pore area (Figure 16A), (ii) apparent density (Figure 16B) and (iii) bulk

density (Figure 16C), compared with the reference paste. Hence, although there is significant inherent variability in the samples and the method itself is being challenged, the mere comparison of results can still provide valid scientific evidences. This is the reason why the MIP results were in good agreement with all other results presented in this paper.

To begin with, nC1 increased the total pore area and porosity [48], in contrast to some other reported results suggesting that organomodified nMt act as nanofillers, reducing the total pore volume [36]. Moreover, nC1, was the only dispersion that caused an increase in total pore area from day 1 to day 90, as also confirmed by the voids observed by FESEM. This could explain the lower than the reference paste's compressive strength of the nC1 modified formulations. Both the apparent and bulk density at later ages tend to be the same for the three nMt dispersions and approaching the reference paste. It is interesting to note that the total pore area at day 28 is almost the same for the reference paste and for the nC2 and nC3 modified pastes, however, with the advancement of time, nC2 seems to have decreased the total pore area. It could be assumed that given the time the pozzolanic reaction advanced densifying the microstructure of the paste, possibly through the production of additional ettringite and C–S–H and/or C–A–H, in agreement with the TG analyses.

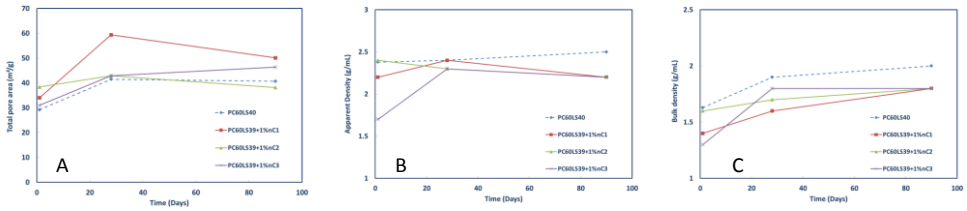


Figure 16. Effect of nMt dispersion on (A) the total pore area, (B) the apparent density and (C) the bulk density of cement pastes

## 4. Conclusions

Based on the results shown in this study, it appears reasonable to assume that the LnS used performed as a pozzolanic material that consumed $Ca(OH)_2$, and that the additional products resulting from this pozzolanic activity, most probably C–S–H, gave rise to improvements in early age strength. Furthermore, these strength improvements were maintained at later ages, for the lower (0.1% and 0.5%) LnS content pastes. Consequently, LnS does not

act simply as an accelerator of reactions but plays a role in the development of an enhanced microstructure. There has been much discussion in the literature on the role of LnS as providing a nucleation point for C–S–H reactions. Given the research reported in this paper and the significant pozzolanic activity observed, it has not been possible to distinguish between the two mechanisms (nucleation sites and pozzolanic activity) in the early ages. It is very likely that the two mechanisms have taken place at the same time.

Judging by the TGA and compressive strength results, it can be assumed that a maximum LnS content has been achieved, particularly with respect to later age performance. It seems reasonable to suggest that LnS additions of less than 0.5% by mass of solids can improve early and late age compressive strength of cement pastes.

Clearly more research is required, but these results potentially provide support to the argument that early-age pozzolanic reactions between LnS and $Ca(OH)_2$ may inhibit pozzolanic reactions involving higher amount of LnS. The reason for this is that nS reacts instantly with $Ca(OH)_2$ produced by cement hydration, forming dense C-S-H. These dense C–S–H areas are formed around unreacted cement particles and $Ca(OH)_2$ particles, acting as ion penetration barriers, impeding homogeneous hydration of the cement paste and consequently further production of $Ca(OH)_2$. As an effect, only a proportion of $Ca(OH)_2$ is available to the pozzolanic reaction, and furthermore, the amount of $Ca(OH)_2$ produced could reduce as nS content increases.

As far as the addition of nMt dispersions is concerned, the results provided a justification for the lower compressive strength attained with the addition of nC1/nC2/nC3 dispersions. The potentials of these nMt dispersions with respect to pozzolanic behaviour and particle packing abilities as expressed in terms of $Ca(OH)_2$ consumption, ettringite and C–S–H production, density and porosity were also discussed. Although past research suggests that nanomontmorillonite exhibits limited pozzolanic activity and need to be calcined when nanomontmorillonite is intercalated or exfoliated it was proven that it can, indeed, act as a pozzolanic addition in cementitious nanocomposites, pushing the envelope of cement science further by suggesting a new range of nanoparticles to be broadly investigated for tailored uses.

The following improvements should be considered in future research with nano-Montmorillonites:

a) the addition of superplasticizers

b) the use of nano-fluidic droplets for the better dispersion of the nanoparticles within the paste

c) different compaction methods aiming at greater homogeneity and limited air voids and

d) various curing methods

## 5. Acknowledgments

The Author acknowledges the European Commission funding (FIBCEM project, grant Number 262954) and all partners are thanked for their input and for the supply of materials. The author would like to thank Dr Kevin Paine, Reader at the University of Bath, BRE Centre for Innovative Construction Materials for the comments provided and also the Department of Chemical Engineering at the University of Bath for the use of the TG analyser.

## 6. Conflict of Interest

There is no 'conflict of interest' related to this work.

## 7. References

[1] CEN, Cement - Part 1: Composition, specifications and conformity criteria for common cements, EN 197-1:2 (2000) 29.

[2] A.A. Elgalhud, R.K. Dhir, G. Ghataora, Limestone addition effects on concrete porosity, Cem. Concr. Compos. 72 (2016) 222–234. doi:10.1016/J.CEMCONCOMP.2016.06.006.

[3] S. Tsivilis, E. Chaniotakis, E. Badogiannis, G. Pahoulas, A. Ilias, A study on the parameters affecting the properties of Portland limestone cements, Cem. Concr. Compos. 21 (1999) 107–116. doi:https://doi.org/10.1016/S0958-9465(98)00031-6.

[4] F. Lollini, E. Redaelli, L. Bertolini, Effects of portland cement replacement with limestone on the properties of hardened concrete, Cem. Concr. Compos. 46 (2014) 32–40.

doi:https://doi.org/10.1016/j.cemconcomp.2013.10.016.

[5] M. Zajac, A. Rossberg, G. Le Saout, B. Lothenbach, Influence of limestone and anhydrite on the hydration of Portland cements, Cem. Concr. Compos. 46 (2014) 99–108. doi:https://doi.org/10.1016/j.cemconcomp.2013.11.007.

[6] G.D. Moon, S. Oh, S.H. Jung, Y.C. Choi, Effects of the fineness of limestone powder and cement on the hydration and strength development of PLC concrete, Constr. Build. Mater. 135 (2017) 129–136. doi:10.1016/J.CONBUILDMAT.2016.12.189.

[7] J. Calabria-Holley, S. Papatzani, Effects of nanosilica on the calcium silicate hydrates in Portland cement-fly ash systems, Adv. Cem. Res. 26 (2014) 1–14.

[8] S. Papatzani, K. Paine, Polycarboxylate/nanosilica-modified quaternary cement formulations – enhancements and limitations, Adv. Cem. Res. 30 (2018) 256–269. doi:10.1680/jadcr.17.00111.

[9] S. Papatzani, K. Paine, Dispersed Inorganic or Organomodified Montmorillonite Clay Nanoparticles for Blended Portland Cement Pastes: Effects on Microstructure and Strength, in: K. Sobolev, S.P. Shah (Eds.), Nanotechnol. Constr. Proc. NICOM5, Springer International Publishing, 2015: pp. 131–139. doi:10.1007/978-3-319-17088-6_16.

[10] F. Soleymani, Optimum content of SiO2 nanoparticles in concrete specimens, J. Am. Sci. 8 (2012) 432–437. http://www.americanscience.org.

[11] Qing Ye, Z. Zhang, D. Kong, R. Chen, Influence of nano-SiO2 addition on properties of hardened cement paste as compared with silica fume, Constr. Build. Mater. 21 (2007) 539–545. doi:10.1016/j.conbuildmat.2005.09.001.

[12] H. Li, H. Xiao, J. Yuan, J. Ou, Microstructure of cement mortar with nano-particles, Compos. Part B Eng. 35 (2004) 185–189. doi:http://dx.doi.org/10.1016/S1359-8368(03)00052-0.

[13] S. Papatzani, Effect of nanosilica and montmorillonite nanoclay particles on cement hydration and microstructure, Mater. Sci. Technol. 32 (2016) 138–153. doi:10.1179/1743284715Y.0000000067.

[14] S. Papatzani, K. Paine, J. Calabria-Holley, A comprehensive review of the models on the nanostructure of calcium silicate hydrates, Constr. Build. Mater. 74 (2015) 219–234. doi:http://dx.doi.org/10.1016/j.conbuildmat.2014.10.029.

[15] Y. Xi, Synthesis, Characterisation and Application of Organoclays, Queensland University of Technology, 2006.

[16] L.A. Utracki, Clay-containing polymeric nanocomposites, iSmithers Rapra Publishing, 2004.

[17] A.A. Sapalidis, F.K. Katsaros, N.K. Kanellopoulos, PVA/Montmorillonite Nanocomposites: Development and Properties, in: J. Cuppoletti (Ed.), Nanocomposites Polym. with Anal. Methods, InTech, 2011. doi:10.5772/18217.

[18] S.G. Jahromi, B. Andalibizade, S. Vossough, Engineering properties of nanoclay modified asphalt concrete mixtures, Arab. J. Sci. Eng. Sect. B Eng. 35 (2010) 90. http://sfxhosted.exlibrisgroup.com/bath?sid=google&auinit=SG&aulast=Jahromi&atitle=Engineering properties of nanoclay modified asphalt concrete mixtures&title=Arabian journal for science and engineering. Section B%3A Engineering&volume=35&issue=1B&date=2010&spage=90&issn=1319-8025.

[19] S. Papatzani, K. Paine, Inorganic and organomodified nano-montmorillonite dispersions for use as supplementary cementitious materials - A novel theory based on nanostructural studies, Nanocomposites. 3 (2017) 2–19. doi:10.1080/20550324.2017.1315210.

[20] J. Wheeler, S. Polak, The use of Nanomaterials in UK Universities : an overview of occupational health and safety, (2013) 48.

[21] J. Freeland, J. Hulme, D. Kinninson, A. Mitchell, P. Veitch, R. Aitken, et al., Working Safely with Nanomaterials in Research & Development, (2012) 1–44. http://www.gla.ac.uk/media/media_259466_en.pdf.

[22] Health and Sefety Executive, Review of the adequacy of current regulatory regimes to secure effective regulation of nanoparticles created by nanotechnology, (2006) 22.

[23] S. Aldrich, Nanosilica prices, (n.d.). https://www.sigmaaldrich.com/catalog/search?term=colloidal+silica &interface=All&N=0&mode=match partialmax&lang=en&region=GB&focus=product (accessed January 15, 2018).

[24] J. Calabria-Holley, S. Papatzani, B. Naden, J. Mitchels, K. Paine, Tailored montmorillonite nanoparticles and their behaviour in the alkaline cement environment, Appl. Clay Sci. 143 (2017) 67–75. doi:http://dx.doi.org/10.1016/j.clay.2017.03.005.

[25] S. Papatzani, K. Paine, J. Calabria-Holley, The effect of the addition of nanoparticles of silica on the strength and microstructure of blended Portland cement pastes, Boston, May 12-15, Int. Concr. Sustain. Conf. (2014). http://www.nrmcaevents.org/?nav=display&file=648.

[26] S. Papatzani, K. Paine, Polycarboxylate / nanosilica modified quaternary cement formulations - enhancements and limitations, Adv. Cem. Res. 30 (2018) 256–269. doi:10.1680/jadcr.17.00111.

[27] J. Calabria-Holley, K. Paine, S. Papatzani, Effects of nanosilica on the calcium silicate hydrates in Portland cement–fly ash systems, Adv. Cem. Res. 27 (2015) 187–200. doi:10.1680/adcr.13.00098.

[28] J. Zhang, G.W. Scherer, Comparison of methods for arresting hydration of cement, Cem. Concr. Res. 41 (2011) 1024–1036.

[29] G. Bye, P. Livesey, L. Struble, Portland Cement, ICE Publishing, 2011. doi:10.1680/pc.36116.

[30] K. De Weerdt, M. Ben Haha, G. Le Saout, K.O. Kjellsen, H. Justnes, B. Lothenbach, Hydration mechanisms of ternary Portland cements containing limestone powder and fly ash, Cem. Concr. Res. 41 (2011) 279–291. doi:http://dx.doi.org/10.1016/j.cemconres.2010.11.014.

[31] С. Папатзани, К. Пэйн, Д. Калабрия-Холли, Прочность и микроструктура цементного камня с добавками коллоидного SiO2 (Strength and microstructure of colloidal nanosilica enhanced cement pastes (In Russian)), Цемент и Его Применение (Cement Its Appl. 4 (2014) 80–85. http://www.cemcom.ru/2014_4%0D.

[32] S. Tsivilis, E. Chaniotakis, G. Kakali, G. Batis, An analysis of the properties of Portland limestone cements and concrete, Cem. Concr.

Compos. 24 (2002) 371–378. doi:https://doi.org/10.1016/S0958-9465(01)00089-0.

[33] A.A. Ramezanianpour, E. Ghiasvand, I. Nickseresht, M. Mahdikhani, F. Moodi, Influence of various amounts of limestone powder on performance of Portland limestone cement concretes, Cem. Concr. Compos. 31 (2009) 715–720. doi:10.1016/J.CEMCONCOMP.2009.08.003.

[34] M.S. Meddah, M.C. Lmbachiya, R.K. Dhir, Potential use of binary and composite limestone cements in concrete production, Constr. Build. Mater. 58 (2014) 193–205. doi:https://doi.org/10.1016/j.conbuildmat.2013.12.012.

[35] A. Marzouki, A. Lecomte, A. Beddey, C. Diliberto, M. Ben Ouezdou, The effects of grinding on the properties of Portland-limestone cement, Constr. Build. Mater. 48 (2013) 1145–1155. doi:https://doi.org/10.1016/j.conbuildmat.2013.07.053.

[36] W.Y. Kuo, J.S. Huang, C.H. Lin, Effects of organo-modified montmorillonite on strengths and permeability of cement mortars, Cem. Concr. Res. 36 (2006) 886–895.

[37] N.C. Collier, Transition and decomposition temperatures of cement phases - a collection of thermal analysis data, Ceram. - Silikaty. 60 (2016) 338–343. doi:10.13168/cs.2016.0050.

[38] V.G. Papadakis, Effect of fly ash on Portland cement systems: Part I. Low-calcium fly ash, Cem. Concr. Res. 29 (1999) 1727–1736. doi:http://dx.doi.org/10.1016/S0008-8846(99)00153-2.

[39] R.M.H. Lawrence, T.J. Mays, P. Walker, D. D'Ayala, Theuse of tg to measure different concentrations of lime in non-hydraulic limemortars, J. Therm. Anal. Calorim. 85 (2006) 377–382. doi:10.1007/s10973-005-7302-7.

[40] P. Hou, J. Qian, X. Cheng, S.P. Shah, Effects of the pozzolanic reactivity of nanoSiO2 on cement-based materials, Cem. Concr. Compos. (n.d.). doi:http://dx.doi.org/10.1016/j.cemconcomp.2014.09.014.

[41] S.P. Shah, P. Hou, M.S. Konsta-Gdoutos, Nano-modification of cementitious material: toward a stronger and durable concrete, J.

Sustain. Cem. Mater. (2015) 1–22. doi:10.1080/21650373.2015.1086286.

[42] B. Lothenbach, G. Le Saout, E. Gallucci, K. Scrivener, Influence of limestone on the hydration of Portland cements, Cem. Concr. Res. 38 (2008) 848–860. doi:http://dx.doi.org/10.1016/j.cemconres.2008.01.002.

[43] T.D. Dyer, R.K. Dhir, Hydration reactions of cement combinations containing vitrified incinerator fly ash, Cem. Concr. Res. 34 (2004) 849–856. http://www.scopus.com/inward/record.url?eid=2-s2.0-1942532881&partnerID=40&md5=a58c5a72e1817231d28f9cb615bd3e2a.

[44] S. Papatzani, Nanotechnologically modified cements: Effects on hydration, microstructure and physical properties, University of Bath, 2014.

[45] T.P. Chang, J.Y. Shih, K.M. Yang, T.C. Hsiao, Material properties of Portland cement paste with nano-montmorillonite, J. Mater. Sci. 42 (2007) 7478–7487.

[46] X. He, X. Shi, Chloride permeability and microstructure of Portland cement mortars incorporating nanomaterials, Transp. Res. Rec. J. Transp. Res. Board. 2070 (2008) 13–21.

[47] P. Hosseini, R. Hosseinpourpia, A. Pajum, M.M. Khodavirdi, H. Izadi, A. Vaezi, Effect of nano-particles and aminosilane interaction on the performances of cement-based composites: An experimental study, Constr. Build. Mater. 66 (2014) 113–124. doi:http://dx.doi.org/10.1016/j.conbuildmat.2014.05.047.

[48] S. Papatzani, S. Grammatikos, B. Adl-Zarrabi, K. Paine, Pore-structure and microstructural investigation of organomodified/Inorganic nano-montmorillonite cementitious nanocomposites, in: Am. Inst. Phys., 2018: p. 030004. doi:10.1063/1.5034328.

[49] S. Diamond, Mercury porosimetry: An inappropriate method for the measurement of pore size distributions in cement-based materials, Cem. Concr. Res. 30 (2000) 1517–1525.

[50] A.B. Abell, K.L. Willis, D.A. Lange, Mercury intrusion porosimetry and image analysis of cement-based materials, J. Colloid Interface Sci.

211 (1999) 39–44.

Appendix A.

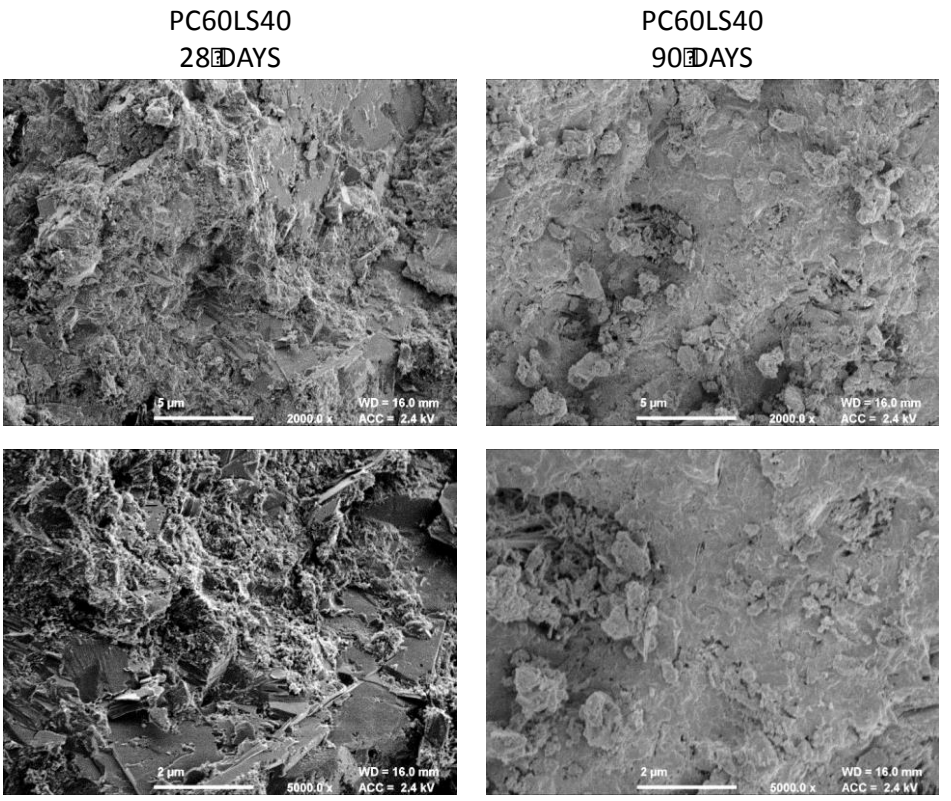


Appendix Figure 1. PC60LS40 at 28D at 28D and at 90D at different magnifications

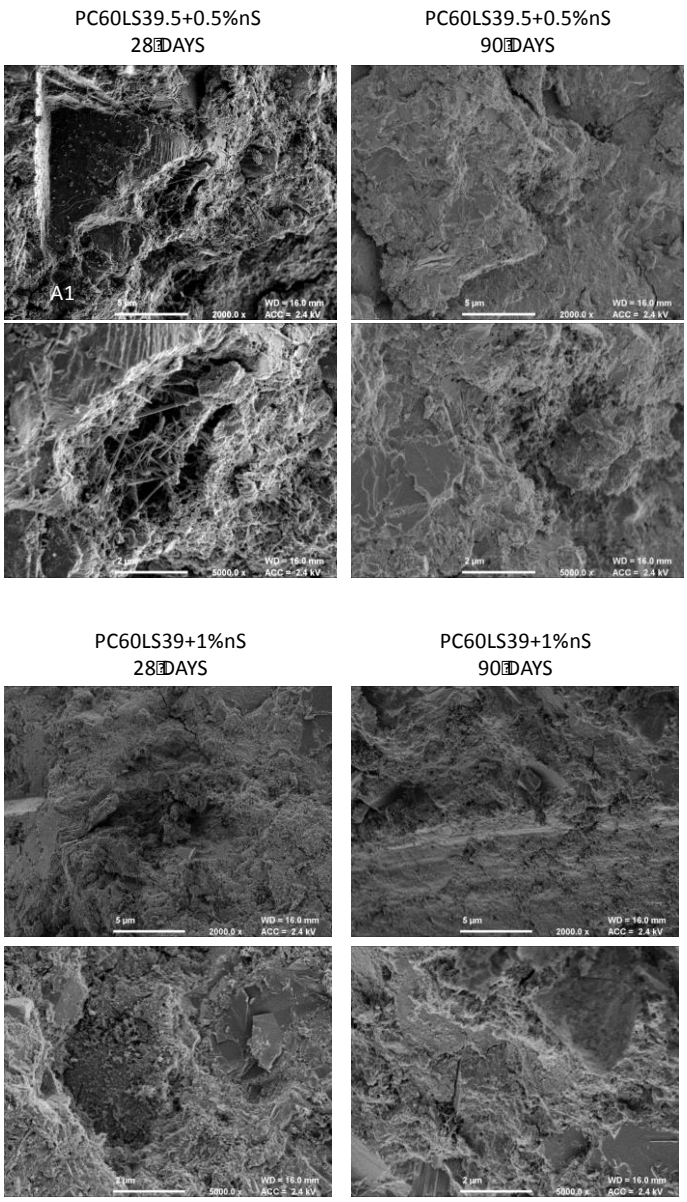


Appendix Figure 2. PC60LS39.5+ 0.5%LnS at 28D and PC60LS39+ 1.0%LnS at 28D and at 90D at different magnifications

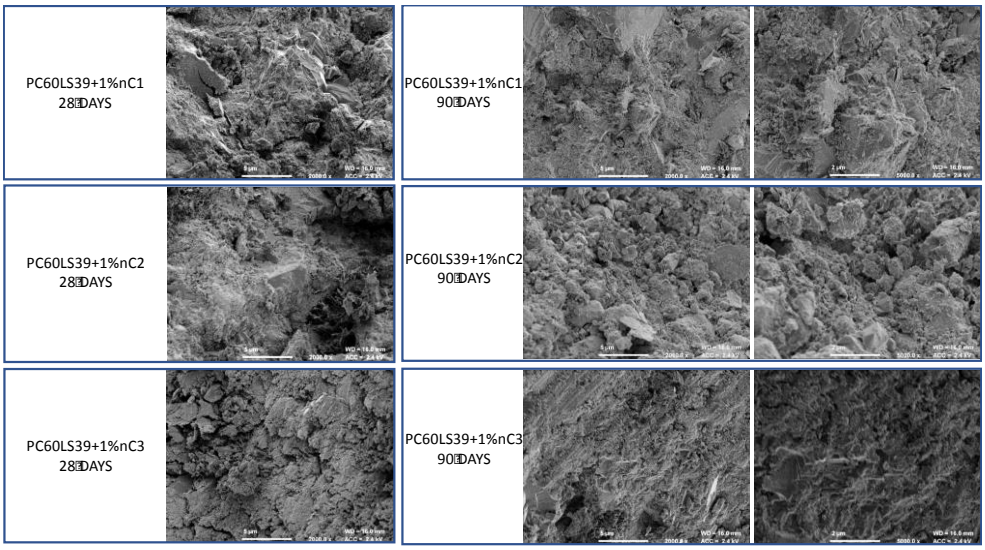


Appendix Figure 3. PC60LS39+ 1%nC1/nC2/nC3 at 28D and at 90D at different magnifications